

# Removal of Diazinon Pesticide Using Amino-silane Modified Magnetite Nanoparticles from Contaminated Water

Atena Naeimi<sup>1,\*</sup>, Mahboubeh Saeidi<sup>2</sup> and Nasr Boroomad<sup>3</sup>

<sup>1</sup>Department of Chemistry, Faculty of science, University of Jiroft, Jiroft, Iran.

<sup>2</sup>Department of Chemistry, Vali-e-Asr University of Rafsanjan, Rafsanjan, Iran.

<sup>3</sup>Faculty of Agriculture, Department of Chemistry, University of Jiroft, Jiroft, Iran.

(\*) Corresponding author: a.naeimi@ujiroft.ac.ir

(Received: 26 September 2016 and Accepted: 04 September 2017)

## Abstract

A magnetically recoverable adsorbent has been prepared by silica-coated magnetic nanoparticles through an amine functionality (ASMNPs). The ASMNPs were characterized by XRD, TEM, SEM, and FT-IR spectroscopy. It was used as an efficient and economical adsorbent for removing O, O-Diethyl O-[4-methyl-6-(propan-2-yl) pyrimidin-2-yl] phosphorothioate (diazinon) from contaminated water through batch experiments. The results were shown that 84% of diazinon was removed after 30 min. The experimental data of the adsorption kinetics were well described by Pseudo-second-order kinetic model ( $R^2 > 0.99$ ), and Equilibrium adsorption data could be better fitted with the Freundlich isotherm ( $R^2 > 0.99$ ). The standard free energy change ( $\Delta G^\circ$ ) and standard enthalpy change ( $\Delta H^\circ$ ) were indicated that this system is a spontaneous and exothermic process.

**Keywords:** Magnetic, Adsorption, Spectrophotometry, Pesticides, Water.

## 1. INTRODUCTION

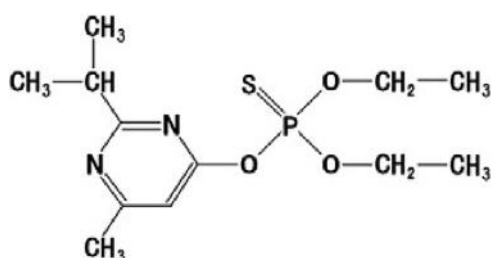
Nanomaterials have shown superior adsorption capacities in the removal of diverse range of chemical contaminants and aromatic solutes due to their shapes with high aspect ratio and provision of large external surface area [1, 2]. The mobility of nanoparticles in solution is high and the whole volume can be quickly scanned with small amounts of nanomaterials due to their small size [3-4]. Therefore, advances in nanotechnology and engineering suggest that many of the current problems involving water quality could be resolved or greatly diminished by using nanoabsorbent. From environmental point of view, iron oxide separation offers advantages because of the easy recovery of the absorbent without filtration or centrifugation [5-6].

In parallel, the use of large quantities of insecticides and pesticides in agriculture activities is one of the main causes of pollution of surface and ground water [7]. Since the majority of organic pesticides are

non-degradable and carcinogenic, they are considered as a powerful category of water contaminants [8-9]. In fact, 17% of 2.36-billion kg of the world pesticide amount used was insecticides. Hence, the contamination of surface and ground water by insecticides has become a serious environmental problem and the removal of insecticides from water is one of the major environmental concerns these days [10]. Conventional technologies have been used to treat all types of organic and toxic waste by adsorption, biological oxidation, chemical oxidation and incineration [11-12]. From an economic point of view, adsorption is simple, fast, real applicable technique [13]. Diazinon was selected as an organophosphate insecticide and volatile insecticide greatly applied to eliminate flies and ticks, especially *O. tholozaniticus*. Low concentrations of diazinon (even 350 ng.L<sup>-1</sup>) can be highly toxic to aquatic organisms [14-16]. It has been found that fatal human

doses are in the range of between 90 and 444 mgKg<sup>-1</sup>. While, this toxin is widely used in farms and its residue could be found in underground waters and rivers and high residual level had been detected in vegetables. It is considered as a major concern for groundwater and drinking water because it is relatively water soluble, nonpolar and moderately mobile. Therefore, it is essential to use effective chemical and biological methods for treatment of wastewaters containing diazinon [17-20]. The structure of diazinon is presented in scheme1.

We recently reported the removal of pyrene and related aromatic hydrocarbons by the several novel complexes based catalyst systems and also friendly environmental oxidation of alcohols to aldehydes and ketons [19-24]. In continuing our work, the amino modified core-shell magnetic nanoparticles were synthesized and used as an efficient adsorbent for the removal of pesticide from aqueous solutions. Optimization of adsorption of diazinon by the classical method involves changing one independent variable (i.e. adsorbent dosages, pH, initial diazinon concentration, contact time, temperature) while maintaining all others at a fixed level which is extremely time consuming and expensive for a large number of variables. To overcome this difficulty, experimental factorial design and response methodology can be employed to optimize the adsorption of diazinon. The objective of the present study is to optimize adsorption of diazinon in aqueous solution onto pretreated *S. cerevisiae* in a batch experiment. For better understanding of adsorption, kinetic, isotherm, and thermodynamic were evaluated.



**Scheme 1.** The structure of *O, O*-Diethyl *O* [4-methyl-6-(propan-2-yl)pyrimidin-2-yl] phosphorothioate( diazinon).

## 2. EXPERIMENTAL

### 2.1 Materials and Methods

Analytical grade diazinon for the experiment was purchased from Fluka Co. (Germany). A diazinon stock solution of 40 mg/L was prepared in distilled water and kept in a refrigerator at 4 °C until use. All other chemicals used, were as analytical grade and were purchased from Merck Co. (Germany). Standard solutions and working solutions were prepared by appropriate dilution of the stock solutions. IR spectra of adsorbent in the 4000–400 cm<sup>-1</sup> regions as KBr disks were recorded on a Thermo SCIENTIFIC model NICOLET iS10 spectrophotometer. HRTEM analysis was performed using HRTEM microscope (Philips CM30). The morphology of the products was determined by using Hitachi Japan, model s4160 Scanning Electron Microscopy (SEM) at accelerating voltage of 15 KV.

### 2.2 Synthesis of Amino-silane Modified Magnetic Nanoparticles (ASMNPs)

#### Synthesis of Magnetite Nanoparticles (Fe<sub>3</sub>O<sub>4</sub>, MNP)

A solution of FeCl<sub>2</sub> (5.40 g) and FeCl<sub>3</sub> (2.00 g) in aqueous hydrochloride acid (2.00 M, 25.00 mL) at room temperature was sonicated until the salts dissolved completely. Aqueous ammonia (25%, 40.00 mL) was added slowly over 20 min to the mixture under Ar atmosphere at room temperature followed by stirring about 30 min with mechanical stirrer. The Fe<sub>3</sub>O<sub>4</sub> nanoparticles were separated by external magnet and washed three times with deionized water and ethanol. The final product was obtained after drying under vacuum [25].

#### 2.3 Synthesis of Silica-Coated Magnetite Nanoparticles (SMNP)

The synthesized Fe<sub>3</sub>O<sub>4</sub> suspended in 35.00 mL ethanol and 6 mL deionized water

and sonicated for 15 min. 1.50 mL of tetraethyl orthosilicate was added slowly to the mixture and sonicated for 10 min. Then aqueous ammonia (10%, 1.40 mL) was added slowly over 10 min under mechanical stirrer. The mixture was heated at 40 °C for 12 h. The iron oxide nanoparticles with a thin layer of silica (Fe<sub>3</sub>O<sub>4</sub>@SiO<sub>2</sub>, SMNP) were separated by an external magnet and washed three times with ethanol and dried under vacuum [25].

## 2.4 Amination of Silica-Coated Magnetite Nanoparticles (ASMNP)

10.00 g of dry SMNP powder were mixed with 200.00 mL of toluene to produce a homogeneously mixed solution, followed by sonication the mixture for 30 min. Then 2.50 mL of (3-aminopropyl) triethoxysilane was added under mechanical stirring and the mixture was slowly heated to 105°C and kept at this temperature for 20 h. The final sample (ASMNP) was separated by an external magnet and washed three times with methanol or ethanol and dried under vacuum. The concentrated product stored in refrigerator to use [25]. The magnetite adsorbent was characterized by TEM, SEM, XRD, and FT-IR.

## 2.5 Adsorption Experiments and Analysis

Adsorption of diazinon on ASMNPs was investigated through batch experiments at room temperature. A stock diazinon solution of 40 mg/L was prepared by dissolving 36mL of diazinon in a 1000mL of deionized water. The solution was diluted for different diazinon concentration by deionized water as required working solutions. The initial pH of working solution was adjusted by addition of 2N HCl and 2N NaOH. Batch adsorption experiments were conducted to study the effect of solution pH, initial diazinon concentration and the dosage of ASMNPs. Each experiment was carried out in Erlenmeyer flasks containing 5mg l<sup>-1</sup> diazinon solutions by shaking the flasks at

120rpm for period contact time of 60 min. After shaking, the suspensions were separated by an external magnet. The solutions were carefully decanted to be analyzed using a UV/Vis spectrophotometer, at 236 nm, which was the maximum wavelength for diazinon.

## 2.6 Kinetic Modeling

The adsorption kinetics of diazinon onto ASMNPs to evaluate the controlling mechanism of adsorption process was investigated using two simplified kinetic models including the Lagergren pseudo-first-order and pseudo-second-order, equation 1 and equation 3, respectively.

$$dq_t / dt = k_1(q_e - q_t) \quad (1)$$

Where  $k_1$  is the adsorption rate constant of pseudo-first-order model,  $q_t$  and  $q_e$  are the amount of diazinon adsorbed at time  $t$  (mg g<sup>-1</sup>) and at equilibrium (mg g<sup>-1</sup>) respectively [33]. The linear form of this equation is as follow:

$$\ln(q_e - q_t) = \ln(q_e) - k_1 t \quad (2)$$

A linear plot of  $\ln(q_e - q_t)$  versus  $t$  allows us to determine  $k_1$  and  $q_e$  values from the slope and the intercept of the equation (Figure 9) [27].

The pseudo-second-order kinetic model can be represented in the following form:

$$dq_t / dt = k_2(q_e - q_t)^2 \quad (3)$$

Where  $k_2$  is the equilibrium rate constant of pseudo-second-order model (g mg<sup>-1</sup> min<sup>-1</sup>),  $q_t$  is the amount of diazinon adsorbed at time  $t$  (mg g<sup>-1</sup>) and  $q_e$  is the amount of the diazinon adsorbed at equilibrium (mg g<sup>-1</sup>). The linear form of this equation is as follow:

$$t / q = 1 / k_2 q_e^2 + 1 / q_e t \quad (4)$$

The  $q_e$  and  $k_2$  values of the pseudo-second-order kinetic model can be determined from the slope and the intercept of the plots of  $t/q$  versus  $t$ , respectively (Figure 10) [33]. The adsorption capacity of diazinon onto ASMNPs at a certain time ( $q_t$ ,

mg g<sup>-1</sup>) and at equilibrium (q<sub>e</sub>, mg g<sup>-1</sup>) can be calculated by equation 5 and equation 6, respectively.

$$q_t = V \frac{C_0 - C_t}{m} \quad (5)$$

$$q_e = V \frac{C_0 - C_e}{m} \quad (6)$$

Where C<sub>0</sub> (mg L<sup>-1</sup>) is the initial concentration of diazinon, C<sub>e</sub> (mg L<sup>-1</sup>) is the equilibrium concentration of diazinon, C<sub>t</sub> (mg L<sup>-1</sup>) is the concentrations of diazinon at a certain time t, V (L) is the solution volume and m (g) is the mass of ASMNPs [34]. The kinetic parameters including the pseudo-first-order rate constant k<sub>1</sub> and the pseudo-second-order rate constant k<sub>2</sub>, calculated equilibrium adsorption amount q<sub>e,cal</sub> and experimental equilibrium adsorption amount q<sub>e,exp</sub> and regression coefficients (R<sup>2</sup>).

## 2.7 Adsorption Isotherms

The amount of solute adsorbed per unit weight of adsorbent as a function of the equilibrium concentration in the bulk solution at constant temperature was presented by an adsorption isotherm [31]. In our study, Langmuir, Freundlich and Temkin isotherms were used to describe the adsorption behavior of diazinon onto ASMNPs. The Langmuir adsorption isotherm is based on the assumption that maximum adsorption corresponds to a saturated monolayer of solute molecules on the adsorbent surface, with no lateral interaction between the adsorbed molecules [28]. The Langmuir isotherm can be expressed as follow:

$$q_e = Q_0 k_L C_e / 1 + k_L C_e \quad (7)$$

Where Q<sub>0</sub> and k<sub>L</sub> are the Langmuir constants related to the adsorption capacity and energy of adsorption, respectively [55]. The linear expression of the Langmuir isotherm is as follow:

$$C_e / q_e = 1 / k_L q_{\max} + C_e / q_{\max} \quad (8)$$

Where q<sub>e</sub> (mg g<sup>-1</sup>) and C<sub>e</sub> (mg L<sup>-1</sup>) are the amounts of adsorbed diazinon per unit mass of ASMNPs and diazinon concentration at equilibrium, respectively. q<sub>max</sub> is the maximum amount of the diazinon per unit mass of adsorbent to form a complete monolayer on the surface bound at high C<sub>e</sub> and k<sub>L</sub> is a constant related to the affinity of the binding sites (L mg<sup>-1</sup>). The Langmuir constants q<sub>max</sub> and k<sub>L</sub> can be determined from the slope and intercept of the plot of specific adsorption (C<sub>e</sub>/q<sub>e</sub>) against the equilibrium concentration (C<sub>e</sub>) (Figure 11) [28, 10]. The essential characteristics of the Langmuir isotherm can be expressed in terms of a dimensionless constant separation factor R<sub>L</sub> that is given as follow:

$$R_L = 1 / k_L C_0 \quad (9)$$

Where k<sub>L</sub> is the Langmuir constant and C<sub>0</sub> is the highest initial diazinon concentration (mg L<sup>-1</sup>). The value of R<sub>L</sub> indicates the type of isotherm to be either favorable (0 < R<sub>L</sub> < 1), linear (R<sub>L</sub> = 1), unfavorable (R<sub>L</sub> > 1), or irreversible (R<sub>L</sub> = 0) [36].

The Freundlich isotherm is an empirical equation employed to describe heterogeneous systems. This isotherm assumed that the stronger binding sites are occupied first and that the binding strength decreases with the increasing degree of site occupation [28, 33]. The Freundlich equation is expressed as:

$$q_e = k_f C_e^{1/n} \quad (10)$$

Where k<sub>F</sub> and n are Freundlich constants with k<sub>F</sub> (mg g<sup>-1</sup> (L/mg)<sup>-1/n</sup>) is the adsorption capacity of the diazinon and n giving an indication of how favorable the adsorption process. The magnitude of the exponent, 1/n, gives an indication of the favorability of adsorption. Values of 1/n < 1 represent favorable adsorption condition [36-37]. The linear form of Freundlich isotherm is shown by equation 11.

$$\ln q_e = \ln k_f + \frac{1}{n} \ln C_e \quad (11)$$

$\ln(q_e)$  was plotted against  $\ln(C_e)$  to determine the constants  $k_F$  and  $n$ . Values of  $k_F$  and  $n$  are calculated from the intercept and slope of the plot (Figure 12) [38].

Temkin and Pyzhev considered the effects of indirect adsorbate/adsorbate interactions on adsorption isotherms. The heat of adsorption of all molecules in the layer would decrease linearly with coverage due to adsorbate/adsorbate interactions [39]. This isotherm can be shown as equation 12:

$$q_e = RT \ln(AC)/b \quad (12)$$

Where  $b$  is the Temkin constant related to heat of adsorption ( $J \text{ mol}^{-1}$ ),  $A$  is the Temkin isotherm constant ( $L \text{ g}^{-1}$ ),  $R$  is the gas constant ( $8.314 \text{ J mol}^{-1} \text{ K}^{-1}$ ), and  $T$  is the absolute temperature (K) [33]. The linear form of Temkin isotherm is as follow:

$$q_e = B \ln A + B \ln C_e \quad (13)$$

Where  $B = RT/b$  [39].  $A$  and  $B$  constants can be determined by plotting  $q_e$  against  $\ln C_e$ .

## 2.8 Thermodynamic of Adsorption

In order to know the nature of diazinon adsorption process, thermodynamic parameters including standard free energy change ( $\Delta G^\circ$ , kJ), standard enthalpy change ( $\Delta H^\circ$ , kJ) and standard entropy change ( $\Delta S^\circ$ ,  $J \text{ K}^{-1}$ ) were determined. These thermodynamic parameters can be calculated as follow:

$$\Delta G^\circ = -RT \ln K \quad (14)$$

$$\Delta G^\circ = \Delta H^\circ - T \Delta S^\circ \quad (15)$$

By combination of equations (14) and (15), we can conclude:

$$\ln K = -\Delta G^\circ / RT = \Delta S^\circ / R - \Delta H^\circ / RT \quad (16)$$

Where  $R$  ( $8.314 \times 10^{-3} \text{ kJ mol}^{-1} \text{ K}^{-1}$ ) is the universal gas constant,  $T$  (K) is the solution temperature, and  $K$  is the equilibrium adsorption constants of the isotherm fits [34]. Using the  $K$  values determined from the adsorption isotherm equations ( $K=q_e/C_e$ ) [27], the corresponding values of  $\Delta G^\circ$  of adsorption can be determined at

different experimental temperatures. According to the equation (15),  $\Delta G^\circ$  is the function of change in enthalpy and entropy of adsorption, so  $\Delta H^\circ$  and  $\Delta S^\circ$  can be determined from the slope and the intercept of the linear plot of  $\ln K$  versus  $1/T$  [33].

## 3. RESULTS AND DISCUSSION

### 3.1 Characterization of ASMNPs

In order to characterization of synthesized nanoparticles, the particle size and morphology of the samples were determined by transmission electron microscopy (TEM), scanning electron microscopy (SEM), powder X-ray diffraction (XRD) and FT-IR spectroscopy. The SEM and TEM images of ASMNPs showed uniformity and spherical morphology of nanoparticles with an average diameter of 10 nm (Figure 1). The crystalline structure of the MNP with a cubic structure was identified with XRD (Figure 2). Figure 3 demonstrates the FT-IR spectra of ASMNPs. The presence of magnetite core in the prepared nanomaterials was confirmed by observation of two bands at around 430–600  $\text{cm}^{-1}$ . The broad peak at about 900–1200  $\text{cm}^{-1}$  assigned to Si-O-Si and Si-OH stretching vibrations showed the silica coating of magnetite nanoparticles. The anchoring of aminopropyl groups on SMNP was confirmed by stretching vibrations appeared at about 2800-3000 and 3423  $\text{cm}^{-1}$  [25].

### 3.2 Adsorption of Diazinon on ASMNPs

#### 3.2.1 The Effect of Initial Concentration of Diazinon

First of all, the initial concentration of diazinon was examined. For this aim, the removal efficiencies (RE) were calculated by following equation, in the presence of constant amount of adsorbent and different concentration of diazinon.

$$\text{Re\%} = ((C_0 - C_e) / C_0) \times 100$$

Where  $C_0$  is the initial concentration of diazinon and  $C_e$  is the concentration of diazinon in equilibrium time.

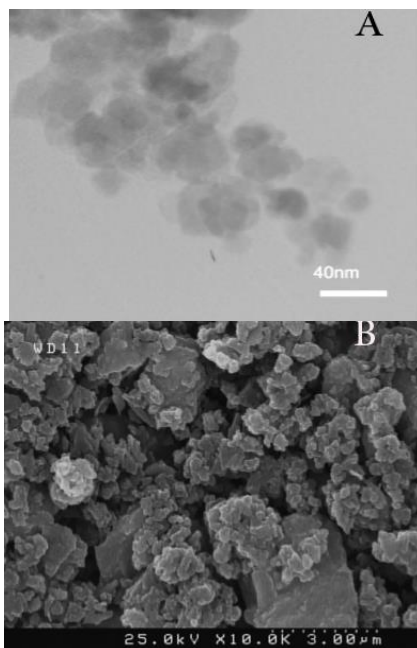


**Figure 1.** TEM (A) and SEM (B) images of ASMNPs.

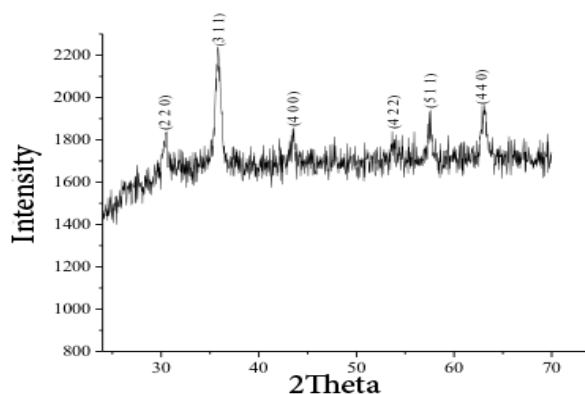


**Figure 2.** XRD patterns of ASMNPs.

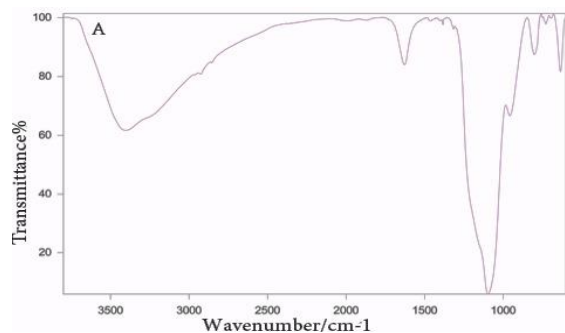


**Figure 3.** The FT-IR of ASMNP.

Finally the RE% was plotted against  $C_0$  and the best removal efficiency was obtained for the initial concentration of  $5 \text{ mg L}^{-1}$  (Figure 4)

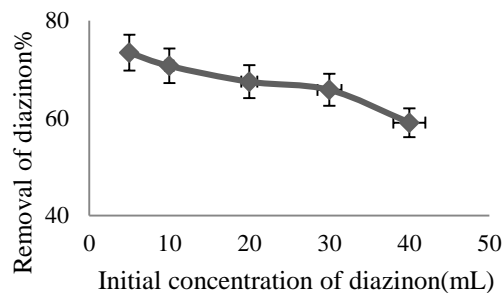


**Figure 4.** The effect of initial concentration of diazinon on the removal efficiency.

### 3.2.2 Effect of Adsorbent Dosage

The adsorbent dosage is an important parameter because this parameter determines the capacity of adsorbent for a given diazinon concentration and also determines adsorbent-adsorbate equilibrium of the system [26]. Therefore the effect of adsorbent dosage in the range of 0.1-20 mg on the diazinon adsorption was studied using a solution containing  $5 \text{ mg L}^{-1}$  diazinon solution. The results of diazinon removal at various ASMNPs dosage were shown in Figure 5. The percentage of removal of diazinon increased from 55.1% at 0.1 mg to 84% at 2.5 mg of adsorbent dosage. The optimum dosage was found to be 2.5 mg. The improvement of diazinon removal with increased dose of ASMNs as an adsorbent can be attributed to the increased adsorbent surface area and availability of active adsorption sites for a fixed number of diazinon molecules in the solution [26-27].

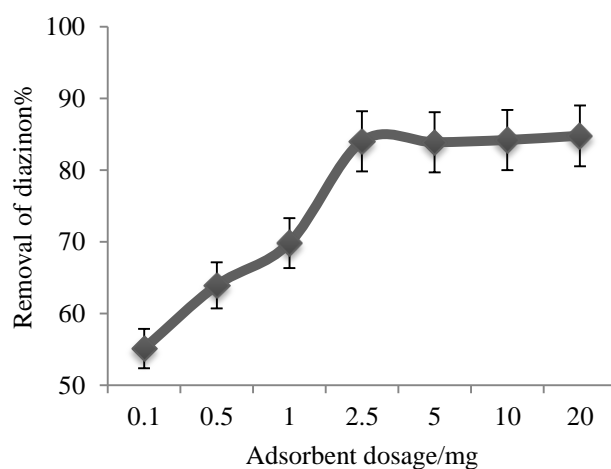


**Figure 5.** Effect of adsorbent dosage on removal of diazinon onto ASMNPs

### 3.2.3. Effect of Solution pH

The effect of pH of water on diazinon adsorption on ASMNs was investigated in the range of 2 to 10. The equilibrium adsorption ( $q_e$ ) was decreased by increasing the pH of water (Figure 6). The behavior suggests that the adsorption was dominated by the interaction between diazinon and adsorbent surface [28]. A greater degree of hydrolysis was observed in pH levels that were acidic [29]. The adsorption of diazinon however, started to increase at a solution pH level over 7. It should be noted that pKa of diazinon is 2.6. The surface of ASMNPs is positively charged at a solution pH level below 7. However, at pH above pKa diazinon molecules dissociate to anionic species [30]. The greater the pH level of the solution above pKa, the higher is the degree of diazinon dissociation, it thereby becomes more negatively charged [31]. In pH of 2, the maximum negative diazinon and positive ASMNPs was observed that best ionic interaction was obtained. The reduction of diazinon adsorption with increased pH level up to 7 can be observed; at a pH level above ASMNPs of 7 the surface of ASMNPs becomes negatively charged and this electrostatically repulsed the diazinon [32].

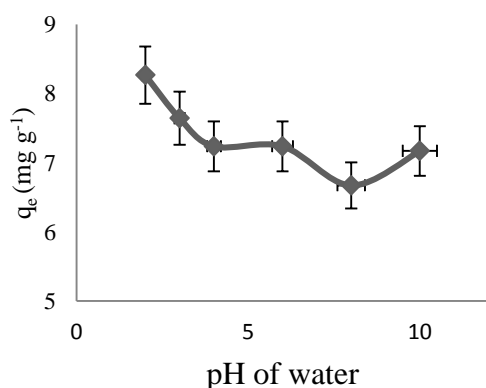


**Figure 6.** Effect of solution pH on removal of diazinon by ASMNPs.

### 3.2.4 Effect of Contact Time

Another important parameter in the adsorption process is the contact time

between adsorbate and adsorbent (Figure 7). At different contact time (2-60min), the adsorption of diazinon on 2.5mg of ASMNPs was performed with initial diazinon concentrations of 5 mg L<sup>-1</sup>. The adsorption process increased rapidly within 30 min and it reaches equilibrium after 30 min. The fast adsorption at the initial stage may be due to a large number of surface sites are available for adsorption. As a result, the remaining vacant surface sites are difficult to be occupied due to formation of repulsive forces between the diazinon molecules on the solid surface and in the bulk phase [26]

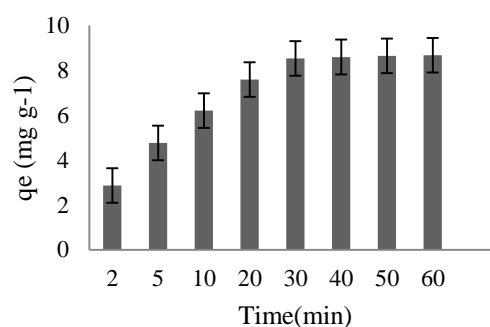


**Figure 7.** Effect of contact time on removal of diazinon by ASMNPs.

### 3.2.5 Effect of Temperature

The effect of temperature on diazinon adsorption onto ASMNPs was carried out at the range of 15°C to 45°C. The amount of equilibrium adsorption of diazinon decreased by the increasing temperature from 15°C to 45°C that indicates an exothermic process (Figure 8). This finding could be due to a tendency for the target molecules to escape from the solid phase to the bulk phase with an increase in temperature of the solution [33].

### 3.2.6 Effect of Water Impurities

The effect of several important water impurities including NaCl and ammonia on the adsorption of diazinon onto ASMNPs was investigated. 0–1.5 mg L<sup>-1</sup> and 0–20 mg L<sup>-1</sup> were used for concentration of NaCl, ammonia and respectively [27]. These results were shown that the percentage of diazinon adsorption improved in the

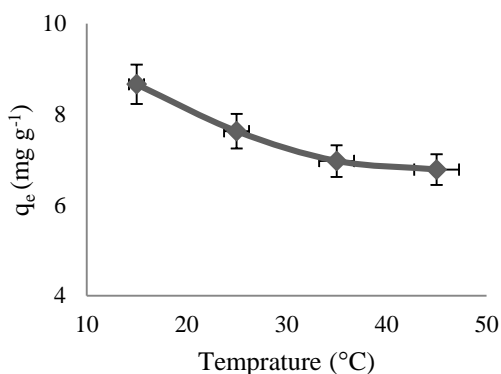


**Figure 8.** Effect of temperature on removal of diazinon onto ASMNPs.

presence of NaCl (Figure 9(A)). It could be due to the electrostatic interaction that is the main mechanism of diazinon adsorption onto ASMNPs. Increased adsorption of organic molecules with a NaCl concentration up to 0.1 M has been reported in other research such as Al-Degs et al [27, 37]. In addition the diazinon adsorption were enhanced in the presence of ammonia (Figure 9(B)). The ammonia molecules in pH<7 have  $\text{NH}_4^+$  and  $\text{OH}^-$  ions and the existent  $\text{OH}^-$  ions in the aqueous medium could form a double layer with negative electric charge around ASMNPs. Therefore the electrostatic interaction between cationic diazinon molecules and negative surface of nanoparticles was confirmed again.

In 2015, F. Chan investigated the effectiveness of chlorine dioxide (CD) to remove phorate and diazinon residues on fresh lettuce and in aqueous solution. At their optimum condition, 60% of diazinon was remained after 20 min [34]. In 2013, K. S. Ryoo reported fly ash, loess, and activated carbon as adsorbent for removal diazinon from water. The equilibrium adsorption times of diazinon by activated carbon and loess were found within 24 h of contact time. Activated carbon showed the best adsorption in the same condition. After 4 hours, Approximately 75-85% of diazinon removed by activated carbon. The adsorption data shows that fly ash is not effective for the adsorption of diazinon [35].

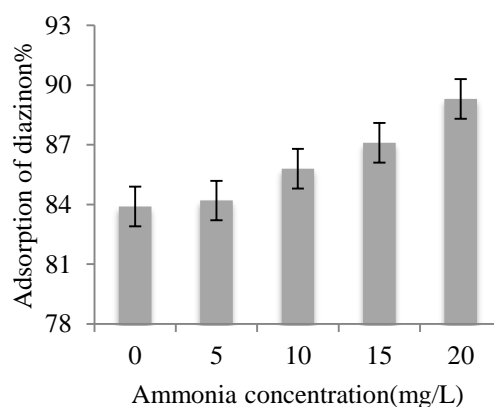
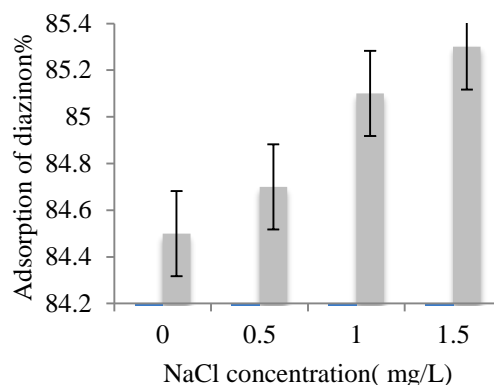


**Figure 9.** The effect of NaCl (0–1.5 mg L<sup>-1</sup>) (A), ammonia (0–20 mg L<sup>-1</sup>) (B) on adsorption of diazinon onto ASMNPs.

Batch removal of diazinon from aqueous solution by granular-activated carbon was reported by M. Fazlzadehdavil in 2014. After 50 min, the highest removal efficiency of 88% for diazinon obtained in 50-min contact time [36]. As our knowledge, the maximum diazinon was removed in the minimum contact time was obtained by ASMNPs (Table 1). On the other hand, TEM and SEM of after adsorption were shown that spherical morphology of adsorbent (Figure 10).

### 3.2.7 Kinetic Modeling, Adsorption Isotherm, and Thermodynamic Adsorption

The kinetic modeling of adsorption of diazinon onto ASMNPs was considered. The conformity between experimental data and the model predicted values is expressed by the correlation coefficients ( $R^2$ ) and comparing the values of  $q_{e,cal}$  and  $q_{e,exp}$ . The relative higher value of  $R^2$  and the lower

value of  $\Delta q$  are the more applicable model to the kinetics of diazinon adsorption onto ASMNPs [33]. The pseudo-second-order model has the higher value of  $R^2$  and the lower value of  $\Delta q$  (Table 2). Thus it seems that the pseudo-second-order kinetic model is more suitable to describe the diazinon adsorption onto ASMNPs. This finding indicates that adsorption capacity is proportional to the number of active sites of ASMNPs [40-41].

**Table 1.** Comparison of adsorption of diazinon.

Entry	Adsorbent	Removal of diazinon%	Time (min)	Ref
1	Chlorine dioxide (CD)	60	20	34
2	Activated carbon	75-87	1440	35
3	Granular-activated carbon	88	50	36
4	Ca-montmorillonite	31	1440	49
5	nanocrystalline magnesium oxides	20-50%	1440	50
6	ASMNPs	84	30	This work

The kinetic modeling of adsorption process was completed by using Bangham's equation evaluating the adsorption is pore-diffusion controlled. Bangham's model equation is generally expressed as [42]

$$\log \log \left( \frac{C_0}{C_0 - q_t \cdot m} \right) = \log \left( \frac{K_B}{2.303 \cdot V} \right) + a \log t \quad (13)$$

Where  $C_0$  is the initial concentration of the adsorbate in solution (mg/L),  $V$  the volume of the solution (L),  $m$  the weight of adsorbent used per liter of solution (g/L),  $q_t$  (mg/g) the amount of adsorbate retained at time  $t$ , and  $a$ ,  $kb$  are constants.

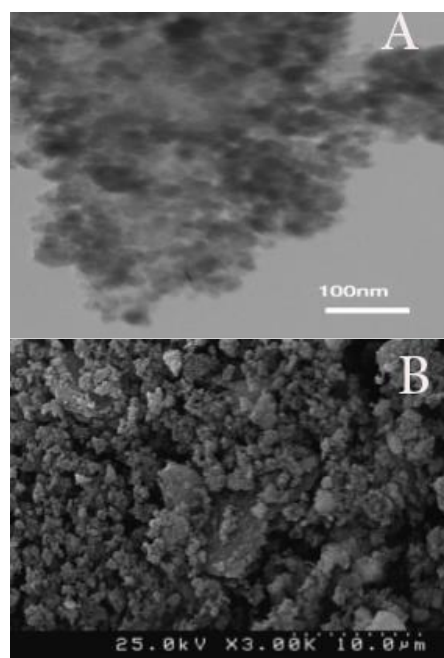


**Figure 10.** The SEM (B) and TEM (A) of ASMNPs after adsorption of diazinon

**Table 2:** The kinetic parameters of diazinon adsorption onto ASMNPs.

pseudo-first-order kinetics model				
$k_1$	$q_{e,exp}$ (mg g <sup>-1</sup> )	$q_{e,cal}$ (mg g <sup>-1</sup> )	$\Delta q$	$R^2$
0.0971	8.54	6.44	2.10	0.9944
pseudo-second-order kinetics model				
$k_2$	$q_{e,exp}$ (mg g <sup>-1</sup> )	$q_{e,cal}$ (mg g <sup>-1</sup> )	$\Delta q$	$R^2$
0.023	8.54	9.33	0.79	0.9992

$\log \log \left( \frac{C_0}{C_0 - q_t \cdot m} \right)$  was plotted against  $\log t$

that  $a$  and  $kb$  constants were calculated from the intercept and slope of the straight line plots of it. The regression coefficients ( $R^2$ ) is 0.9975 that is lower than corresponding value for pseudo-second-order kinetics model (Figure 11).

The Langmuir, Freundlich, and Temkin isotherms as the adsorption isotherms of adsorption of diazinon onto ASMNPs were investigated.

**Table 3.** The information of diazinon adsorption isotherm onto ASMNPs.

Langmuir isotherm			
$R_L$	$k_L$	$q_{max}$	$R^2$
0.18	0.115	112.36	0.9896
Freundlich isotherm			
$1/n$	$k_F$	$R^2$	
0.72	11.92	0.9904	
Temkin isotherm			
A	B	$R^2$	
1.69	20.44	0.9713	

According to Table 3 information, Freundlich isotherm fits quite well with the experimental data because of the value of  $R^2$  in this isotherm is higher ( $R^2 = 0.9904$ ) than the others. A good fit of this equation reflects heterogeneous surface [43]. Moreover the Freundlich model is well known to be a better fit for adsorption into a porous material.

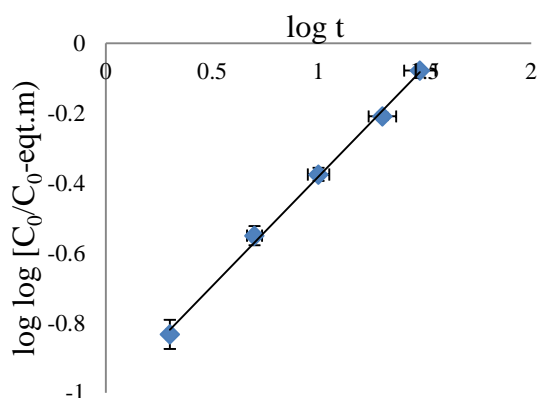


**Figure 11.** The plot of Bangham kinetics model of diazinon adsorption onto ASMNPs.

Thus, these adsorption behaviors seemed to be porous adsorption [10]. The obtained value of Langmuir separation factor,  $R_L$  between 0 and 1 indicates that diazinon adsorption process was favorable. A value of  $1/n$  below one was also confirmed the favorable adsorption process [46].

To understand the better of diazinon adsorption on ASMNPs, the thermodynamic of this process was investigated. All of  $\Delta G^\circ$ ,  $\Delta H^\circ$  and  $\Delta S^\circ$  are

negative during the diazinon adsorption process (Table 4). The negative value of  $\Delta G^\circ$  shows that the adsorption of diazinon onto ASMNPs is a spontaneous and favorable process [27, 40]. The negative value of  $\Delta S^\circ$  indicates a decrease in state of disorderness in the molecules during adsorption of diazinon onto adsorbent, which is due to the binding of molecules with adsorbent surface [46]. The negative value of  $\Delta H^\circ$  shows exothermic nature of the adsorption process [39]. Typically, physisorption which mainly driven by the van der Waals interaction forces, is usually lower than  $20 \text{ kJ mol}^{-1}$ , and electrostatic interaction forces range from 20 to  $80 \text{ kJ mol}^{-1}$  and these kind of interaction forces are, frequently, classified as physisorption; and chemisorption bond strengths can be  $80\text{--}450 \text{ kJ mol}^{-1}$  [39, 47]. According to the obtained value for  $\Delta H^\circ$  ( $-28.62 \text{ kJ mol}^{-1}$ ), can be concluded that the adsorption process of diazinon onto ASMNPs is based on the electrostatic interactions.

**Table 4.** The thermodynamic information of diazinon adsorption onto ASMNPs

Solution tempera ture (K)	K (mL g <sup>-1</sup> )	$\Delta G^\circ$ (kJ mol <sup>-1</sup> )	$\Delta H^\circ$ (kJ mol <sup>-1</sup> )	$\Delta S^\circ$ (J (K mol) <sup>-1</sup> )
288	13.13	-0.32		
298	6.49	-0.39	-28.62	-94.73
308	4.64	-0.45		
318	4.25	-0.54		

Finally, in order to investigate the applicability of the proposed method for removal of diazinon in water samples, adsorption tests were performed on the tap, mineral and well water samples spiked with diazinon ( $5 \text{ mg L}^{-1}$ ). The obtained results are presented in Table 5. A low amount of ASMNPs (2.5 mg) could remove diazinon from aqueous solution at relatively short contact time (30 min) with the acceptable percentage. These findings demonstrate the feasibility of amino modify magnetite nanoparticles (ASMNPs) to removal of diazinon from real contaminated water samples. However, mineral waters consists various ions such as sulphate, chloride,

carbonate, bicarbonate and nitrate that they can reduce the diazinon adsorption on the ASMNPs. In fact, active sites of ASMNPs can be blocked by these ions, which may deactivate for desire pesticide [8].

**Table 5.** The removal of diazinon by ASMNPs from spiked water samples

Water sample	C <sub>0</sub> (mg L <sup>-1</sup> )	C <sub>e</sub> (mg L <sup>-1</sup> )	%R
Tap water	5	1.45	71.61
Mineral water	5	0.83	82.27

### 3.2.8 Adsorption Mechanism of Diazinon on the ASMNPs

Diazinon shows different behavior from two sides, thiophosphate side (dia-OOS) and aromatic side (dia-Ar) when is adsorbed on the ASMNPs [48]. In fact, diazinon was adsorbed on amino-silane modified magnetic nanoparticles by strong bound to adsorbent and its mobility was reduced greatly [49]. ASMNPs did not release diazinon after stirring with fresh and clearly demonstrates that the phenomenon is a chemical adsorption. In order to elucidate the role of NH<sub>2</sub> of ASMNPs groups in adsorption of diazinon, Fe<sub>3</sub>O<sub>4</sub>, Fe<sub>3</sub>O<sub>4</sub>@SiO<sub>2</sub>, Fe<sub>3</sub>O<sub>4</sub>@SiO<sub>2</sub>-NH<sub>2</sub>, carboxylated multiwall carbon nanotubes, and hydroxylated multiwall carbon nanotubes were used to investigate their ability in adsorption of it. 50, 24, 84, 14, and 20 were percentage of diazinon adsorption in optimized condition (pH=2) and the best adsorption process was performed using ASMNPs. In the other hand, it is well known that diazinon is quite stable in basic media. Therefore, it can have strong bound with ASMNPs via amin group on their surface. FT-IR of ASMNPs, after adsorption, was shown the selected bond relating to diazinon. The bond corresponding to P=S stretching vibration of diazinon was observed at 651 cm<sup>-1</sup> [50]. 977 cm<sup>-1</sup> overlapped with ASMNPs and did not disclose further information. Appearance of new band 1561 and 1467 cm<sup>-1</sup> is relate to diazinon [50]. A proposed mechanism for adsorption of diazinon on ASMNPS is illustrated in Scheme 2.

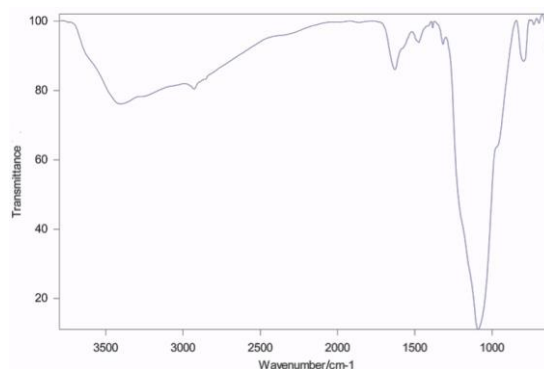
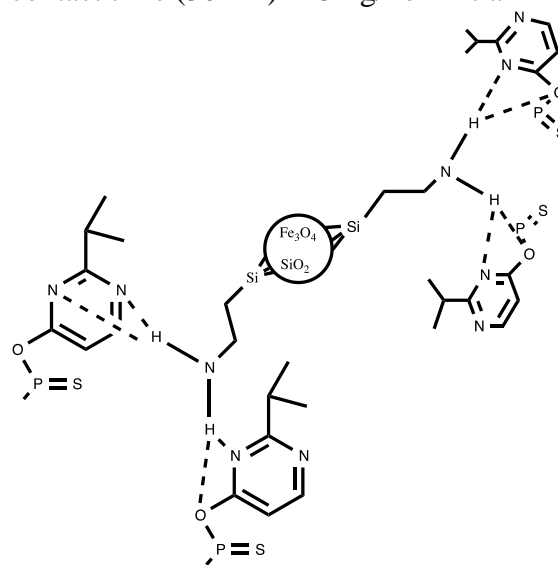


**Figure 12.** FT-IR of ASMNPs after adsorption of diazinon.

## 4. CONCLUSION

The prepared amino modified magnetic nanoparticles was used an absorbent in removal diazinon from water. Adsorption was determined by batch method, which is simple and easy to perform by UV-Vis spectrophotometry at 236 nm. At the present of 2.5mg of ASMNPs, 84% of diazinon was removed after relatively short contact time (30min) in 5mg/l of initial



**Scheme 2.** Proposed mechanism for adsorption of diazinon on the ASMNPs

diazinon concentration. The effect of NaCl and ammonia were considered as important water impurities, in the range of those commonly found in polluted water were investigated. In the presence of NaCl and ammonia, the adsorption of diazinon was improved. The kinetic consideration of

diazinon adsorption is well described by Pseudo-second-order kinetic model and equilibrium adsorption data was fitted with Freundlich isotherm. It should be noted that all the thermodynamic parameters such as  $\Delta G^\circ$  and  $\Delta H^\circ$  were determined and negative values of them were shown a spontaneous and exothermic adsorption process. In order to verify the applicability of the proposed method the same removal procedure were

performed on the tap, mineral, and well water samples spiked with diazinon.

#### ACKNOWLEDGEMENT

We are thankful to University of Jiroft and Vali-e-Asr University of Rafsanjan Research Council for their support on this work.

This study/research was supported by University of Jiroft under the grant no. 3813-93-12.

#### REFERENCES

1. Ren, X., Chen, C., Nagatsu, M., Wang, X., (2011). "Carbon nanotubes as adsorbents in environmental pollution management: A review", *Chem. Eng. J.*, 170: 395-410.
2. Golkhah, S., Mousavi Z. H., Shirkhanloo, H., Khaligh, A., (2017). "Removal of Pb(II) and Cu(II) Ions from Aqueous Solutions by Cadmium Sulfide", *Nanoparticles Int. J. Nanosci. Nanotechnol.*, 13: 105-117.
3. Tiwari, D. K., Behari, J., Sen, P., (2008). "Application of Nanoparticles in Waste Water", *Treatment World Appl. Sci. J.*, 3: 417-433.
4. Sanchez, A., Recillas, S., Font, X., Casals, E., Gonzalez, E., Puentes, V., (2011). "Ecotoxicity of, and remediation with, engineered inorganic nanoparticles in the environment", *Trends Anal. Chem.*, 30: 507-516.
5. Sasaki, T., Tanaka, S., (2011). "Adsorption behavior of some aromatic compounds on hydrophobic magnetite for magnetic separation", *J. Hazard. Mater.*, 196: 327-334.
6. Shin, S., Jang, J., (2007). "Thiol containing polymer encapsulated magnetic nanoparticles as reusable and efficiently separable adsorbent for heavy metal ions", *Chem. Commun.*, 4230-4232.
7. Hidalgo, C., Ríos, C., Hidalgo, M., Salvadó, V., Sancho, J. V., Hernández, F., (2004). "Improved coupled-column liquid chromatographic method for the determination of glyphosate and aminomethylphosphonic acid residues in environmental waters", *J. Chromatogr. A*, 1035: 153-157.
8. Ansari, R., Hassanzadeh, M., Ostovar, f., (2017). "Aresenic removal from water samples using CeO<sub>2</sub>/Fe<sub>2</sub>O<sub>3</sub> nanocomposite", *Int. J. Nanosci. Nanotechnol.*, 13: 335-345.
9. Shirzad-Siboni, M., Jonidi-Jafari, A., Farzadkia, M., Esrafil, A., Gholami, M., (2017). "Enhancement of photocatalytic activity of Cu-doped ZnO nanorods for the degradation of an insecticide: Kinetics and reaction pathways", *Journal of environmental management*, 186: 1-11.
10. Khayat, S. Z., Khayat, S. F., (2013). "Selective Removal of Lead (II) Ion from Wastewater Using Superparamagnetic Monodispersed Iron Oxide (Fe<sub>3</sub>O<sub>4</sub>) Nanoparticles as a Effective Adsorbent", *Int. J. Nanosci. Nanotechnol.*, 9: 109-114.
11. Abdelwahab, O., Amin, N. K., El-Ashtouky, E-SZ., (2009). "Electrochemical removal of phenol from oil refinery wastewater", *J. Hazard. Mater.*, 163: 711-716.
12. Fierro, V., Torné-Fernández, V., Montané, D., Celzard, A., (2008). "Adsorption of phenol onto activated carbons having different textural and surface properties", *Microporous Mesoporous Mater.*, 111: 276.
13. Celis, E., Elefsiniotis, P., Singhal, N., (2008). "Biodegradation of agricultural herbicides in sequencing batch reactors under aerobic or anaerobic conditions", *Water Res.*, 42: 3218-3224.
14. Jonidi-Jafari, A., Gholami, M., Farzadkia, M., Esrafil, A., Shirzad-Siboni, M., (2017). "Application of Ni-doped ZnO nanorods for degradation of diazinon: kinetics and by-products", *Sep. Sci. Technol.*, 1-12.
15. Mohagheghian, A., Karimi, S. A., Ynang, J.K., Shirzad-Siboni, M., (2016) "Photocatalytic degradation of diazinon by illuminated WO<sub>3</sub> nanopowder", *Desalin. Water Treat.*, 57: 8262-8269.
16. Jonidi-Jafari, A., Shirzad-Siboni, M., Yang, J. K., Naimi-Joubani, M., Farrokhi, M., (2015). "Photocatalytic degradation of diazinon with illuminated ZnO-TiO<sub>2</sub> composite", *J. Taiwan Ins. Chem. Eng.*, 50: 100-107.
17. Shirzad-Siboni, M., Khataee, A., Hassani, A., Karaca, S., (2015). "Preparation, characterization and application of a CTAB-modified nanoclay for the adsorption of an herbicide from aqueous solutions: kinetic and equilibrium studies", *C. R. Chim.*, 18: 204-214.
18. Shirzad-Siboni, M., Jafari, S. J., Farrokhi, M., Yang, J. K., (2013). "Removal of phenol from aqueous solutions by activated red mud: "equilibrium and kinetics studies", *Environ. Eng. Res.*, 18: 247-252.
19. Tajic, E., Naeimi, A., Amiri, A., (2017). "Fabrication of iron oxide nanoparticles, and green catalytic application of an immobilized novel iron Schiff on wood cellulose", *Cellulose*, DOI: 10.1007/s10570-017-1615-0.
20. Moreno, A. L., Tejada, D. C., Calbo, J., Naeimi, A., Bermejo, F. A., Orti, E., Perez, E., (2014). "Biomimetic oxidation of pyrene and related aromatic hydrocarbons Unexpected electron accepting abilities of pyrenequinones", *Chem. Commun.*, 50: 9372.

21. Aguiló, J., Naeimi, A., Bofill, R., Bunz, H. M., Liobet, A., Escriche, L., Sala, X., Albericht, M., (2014). "Dinuclear ruthenium complexes containing a new ditopic phthalazin-bis(triazole) ligand that promotes metal-metal interactions", *New J. Chem.*, 38: 1980-1987.
22. Naeimi, A., Saeednia, S., Yoosefian, M., Rudbari, H. A., Nardo, V. M., (2015). "A novel dinuclear schiff base copper complex as an efficient and cost effective catalyst for oxidation of alcohol: synthesis, crystal structure, and theoretical studies", *J. Chem. Sci.*, 127: 1321-1328.
23. Honarmand, M., Naeimi, A., Zahedifar, M., (2017). "Nanoammonium salt: a novel and recyclable organocatalyst for one- pot three- component synthesis of 2- amino- 3- cyano- 4H- pyran derivatives", *J. Iran. Chem. Soc.*, 14:1875-1888.
24. Naeimi, A., Amiri, A., Ghasemi, Z., (2017). "A novel strategy for green synthesis of colloidal porphyrins/silver nanocomposites by *Sesbania sesban* plant and their catalytic application in the clean oxidation of alcohols", *J. Taiwan Ins. Chem. Eng.*, 80: 107-113.
25. Go'ksungur, Y., U' ren, S., Gu' veng, U., (2005). "Biosorption of cadmium and lead ions by ethanol treated waste Baker's yeast biomass". *Bioresour. Technol.*, 96: 103-109.
26. Omri, A., Wali, A., Benzina, M., (2016). "Adsorption of bentazon on activated carbon prepared from *Lawsonia inermis* wood: Equilibrium, kinetic and thermodynamic studies", *Arab. J. Chem.* 9: 1729-1739.
27. Moussavi, G., Hosseini, H.; Alahabadi, A., (2013). "The investigation of diazinon pesticide removal from contaminated water by adsorption onto NH<sub>4</sub>Cl-induced activated carbon", *Chem. Eng. J.*, 214: 172-179.
28. Hameed, B. H., Salman, J. M., Ahmad, A. L., (2009). "Adsorption isotherm and kinetic modeling of 2,4-D pesticide on activated carbon derived from date stones", *J. Hazard. Mater.*, 163: 121-126.
29. Gomaa, H. M., Suffett, I. H., Faust, S. D., (1969). "Kinetics of hydrolysis of diazinon and diazoxon" *Residue Rev.*, 29: 171-190.
30. Saltzman, S., Yaron, B., (1986). "*Pesticides in Soil*", Van Nostrand Reinhold Company, New York, pp.348-351.
31. Salman, J. M., Njku, V. O., Hameed, B. H., (2011). "Adsorption of pesticides from aqueous solution onto banana stalk activated carbon", *Chem. Eng. J.*, 174: 41-48.
32. Ygnqing, A., Miao, C., Qunji, X., Weimin, L., (2007). "Preparation and self-assembly of carboxylic acid-functionalized silica", *J. Colloid Interf. Sci.*, 311: 507-513.
33. Gupta, V., Mohan, D., Sharma, S., (1998). "Removal of Lead from Wastewater Using Bagasse Fly Ash—A Sugar Industry Waste Material", *Separ. Sci. Technol.*, 33: 1331-1343.
34. Chen, Q., Wang, Y., Chen, F., Zhang, Y., Liao, X., (2014). "Chlorine dioxide treatment for the removal of pesticide residues on fresh lettuce and in aqueous solution", *Food Control*, 40: 106-112.
35. Ryoo, K. S., Jung, S. Y., Sim, H., Choi, J. H., (2013). "Comparative Study on Adsorptive Characteristics of Diazinon in Water by Various Adsorbents", *Bull. Korean Chem. Soc.*, 34: 2753-2759.
36. Pirsahaba, M., Dargahia, A., Hazratib, S., Fazlzadehdavil, M., (2014). "Removal of diazinon and 2,4-dichlorophenoxyacetic acid (2,4-D) from aqueous solutions by granular-activated carbon", *Desalin. Water Treat.*, 52: 4350-4355.
37. Al-Degs, Y. S., El-Barghouthi, M. I., El-Sheikh, A. H., Walker, G.M., (2008). "Effect of solution pH, ionic strength, and temperature on adsorption behavior of reactive dyes on activated carbon", *Dyes Pigm.*, 77: 16-23.
38. Humbert, H., Gallard, H., Suty, H., Croué, J. P., (2008). "Natural organic matter (NOM) and pesticides removal using a combination of ion exchange resin and powdered activated carbon (PAC)", *Water Res.* 42: 1635-1643.
39. Bilgili, M. S., Varank, G., Sekman, E., Top, S., Özçimen, D., Yazıcı, R., (2012). "Modeling 4-chlorophenol removal from aqueous solutions by granular activated carbon", *Environ. Model. Assess.*, 17: 289-300.
40. Deng, J., Shao, Y., Gao, N., Deng, Y., Tan, C., Zhou, S., Hu, X., (2012). "Multiwalled carbon nanotubes as adsorbents for removal of herbicide diuron from aqueous solution", *Chem. Eng. J.*, 193-194: 339-347.
41. Yu, Q., Zhang, R. Q., Deng, S. B., Huang, J., Yu, G., (2009). "Sorption of perfluorooctane sulfonate and perfluorooctanoate on activated carbons and resin: Kinetic and isotherm study", *Water Res.*, 43: 1150-1158.
42. Ismi, I., Elaidi, H., Lebkiri, A., Skalli, A., Rifi, E. H., (2014). "Adsorption of Silver (Ag<sup>+</sup>) from aqueous solution by the Sodium Polyacrylate in bead form International", *International Journal of advancements in Reearch and Technology*, 3:121-127.
43. Belhachemi, M., Addoun, F., (2011). "Comparative adsorption isotherms and modeling of methylene blue onto activated carbons", *Appl. Water Sci.* 1: 111-117.
44. Langmuir, I., (1918). "The adsorption of gases on plane surfaces of glass, mica and platinum", *J. Am. Chem. Soc.*, 40: 1361-1403.
45. Hameed, B. H., Mahmoud, D. K., Ahmad, A. L., (2008). "Equilibrium modeling and kinetic studies on the adsorption of basic dye by a low-cost adsorbent: Coconut (*Cocos nucifera*) bunch waste", *J. Hazard. Mater.*, 158: 65-72.
46. Salman J. M., Al-Saad, K. A., (2012). "Adsorption of 2, 4-Dichlorophenoxyacetic acid onto date seeds activated carbon: equilibrium, kinetic and thermodynamic studies", *Int. J. Chem. Sci.*, 10: 677-690.

47. Kuo, C. Y., Wu, C. H., Wu, J. Y., (2008). "Adsorption of direct dyes from aqueous solutions by carbon nanotubes: Determination of equilibrium, kinetics and thermodynamics parameters", *J. Colloid Interface Sci.* 327: 308-315.
48. Farmanzadeh, D., Rezajad, H., (2015). "Adsorption of diazinon and hinosan molecules on the iron-doped boron nitride nanotubes surface in gas phase and aqueous solution; A computational study", DOI: 10.1016/j.apsusc.2015.12.202.
49. Corner, P. K., Matsue, N., Johan, E., Henmi, T., (2014). "Mechanism of Diazinon Adsorption on Iron Modified Montmorillonite", *Am. J. Analyt. Chem.*, 5: 70-76.
50. Armaghan, M., Amini, M. M., (2014) "Adsorption of diazinon and fenitrothion on nanocrystalline magnesium oxides" *Arabian Journal of Chemistry*, DOI: 10.1016/j.arabjc.2014.01.002.